Journal of Inflammation Research

Dovepress
Taylor & Francis Group

Open Access Full Text Article

ORIGINAL RESEARCH

TP-P1-Loaded Thermosensitive Hydrogel Attenuates Rheumatoid Arthritis in a Mouse Model via TLR4/NF-κB Pathway

Fengnan Wang[1,2], Zhongxiao Hu[1,2], Jing Yang[1,2], Chencheng Li[1,2], Weiguang Zhang[1,2], Chenxue Wang[1,2], Shuyi Yu[1,2], Jiaqian Li[1,2], Wenxuan Zhao[1,2], Biqing Chen[1], Xuejun Zhu[1]

[1]Jiangsu Province Hospital of Chinese Medicine, Affiliated Hospital of Nanjing University of Chinese Medicine, Nanjing, Jiangsu, 210029, People's Republic of China; [2]The First Clinical Medical College, Nanjing University of Chinese Medicine, Nanjing, Jiangsu, 210029, People's Republic of China

Correspondence: Biqing Chen; Xuejun Zhu, Jiangsu Province Hospital of Chinese Medicine, Affiliated Hospital of Nanjing University of Chinese Medicine, Nanjing, Jiangsu, 210029, People's Republic of China, Email yfy142@njucm.edu.cn; zhuxuejun@njucm.edu.cn

Purpose: Rheumatoid arthritis (RA) is a chronic autoimmune disease characterized by persistent inflammation, pain, and joint destruction, largely driven by inflammation and oxidative stress. This study explored the therapeutic potential of a thermosensitive hydrogel (TPTH) loaded with TP-P1, a derivative of triptolide, focusing on anti-inflammatory and antioxidant effects.

Methods: A collagen-induced arthritis (CIA) model was established by dual immunization with type II collagen and Freund's adjuvant. Mice were randomized into control, model, dexamethasone (DEX), blank hydrogel, and TPTH groups. After 28 days of intra-articular treatment, arthritis severity was assessed by paw swelling, arthritis scores, and histopathology. Cytokines (IL-6, IL-1β, TNF-α) were measured by RT-qPCR and flow cytometry, oxidative stress markers (MDA, SOD, CAT, GSH) were determined, and TLR4/NF-κB expression was analyzed by Western blotting, immunohistochemistry, and RT-qPCR. Biosafety was evaluated via liver/kidney histology and plasma indices (ALT, AST, BUN, CRE).

Results: TPTH treatment markedly alleviated arthritis symptoms, reducing paw swelling and scores ($p < 0.0001$). It downregulated inflammatory cytokines, improved antioxidant status (SOD, CAT, GSH) and decreased MDA. TPTH also suppressed TLR4 and NF-κB expression, indicating modulation of inflammatory signaling. Importantly, no obvious hepatic or renal toxicity was observed.

Conclusion: TPTH significantly ameliorates inflammation and oxidative stress in CIA mice by modulating the TLR4/NF-κB pathway and shows promise as a safe and effective therapeutic strategy for RA.

Keywords: anti-inflammatory, antioxidant stress capacity, TP-P1-loaded thermosensitive hydrogel, rheumatoid arthritis

Introduction

Rheumatoid arthritis (RA) is a chronic inflammatory autoimmune disease characterized by the breakdown of immune tolerance, abnormal synovial hyperplasia, and progressive joint destruction, ultimately leading to systemic manifestations and long-term disability.[1] Although the precise etiology of RA remains unclear, it is widely accepted that genetic, environmental, and immunological factors contribute synergistically to the onset and progression of the disease.[2] The conventional first-line treatment for RA involves the use of anti-inflammatory agents, such as nonsteroidal anti-inflammatory drugs (NSAIDs), disease-modifying antirheumatic drugs (DMARDs), and biologic agents. These therapies mainly provide symptomatic relief rather than targeting the underlying causes of the disease.[3] However, long-term administration is often associated with serious side effects and high financial burden, which severely limits their prolonged use and overall therapeutic efficacy.[4] For instance, nonsteroidal anti-inflammatory drugs (NSAIDs) are linked to gastrointestinal complications such as dyspepsia, peptic ulceration, and bleeding, as well as cardiovascular risks including myocardial infarction, hypertension, and heart failure.[5] Disease-modifying antirheumatic drugs (DMARDs) may induce adverse events such as nausea, oral ulcers, alopecia, cytopenia, elevated hepatic enzymes, and, albeit rarely, interstitial pneumonitis.[6] Therefore, there is a growing need to develop safer and more effective therapeutic strategies that

Received: 25 June 2025
Accepted: 8 October 2025
Published: 21 October 2025

offer sustained efficacy, particularly those that can target the underlying mechanisms such as inflammation and oxidative stress.[7]

In recent years, hydrogel-based controlled drug delivery systems have attracted considerable attention in tissue engineering and biomedicine due to their ability to provide localized, sustained release of therapeutics. Among them, thermosensitive hydrogels, which remain in a sol state at room temperature and rapidly undergo gelation at body temperature, offer advantages such as minimally invasive administration and prolonged drug retention at the site of inflammation.[8,9] Chitosan (CS), a naturally derived polysaccharide extracted from the shells of crustaceans such as crabs and shrimp, is widely used in hydrogel formulation owing to its excellent biocompatibility, biodegradability, and non-toxicity, making it a promising material for drug delivery applications.

Traditional Chinese Medicine (TCM), as a significant source of complementary and alternative therapies, provides a rich reservoir of bioactive compounds with immunosuppressive and anti-inflammatory properties.[10,11] Tripterygium wilfordii Hook F (TWHF), a well-known medicinal herb in TCM, has been extensively studied for its potent therapeutic effects in autoimmune diseases.[12] Triptolide (TP), a diterpenoid triepoxide and the principal active component of TWHF, has demonstrated robust anti-inflammatory and bone-protective effects in both in vitro and in vivo models.[13–15] However, the clinical application of TP is severely limited by its poor water solubility and considerable toxicity. To address these limitations, we previously synthesized a novel TP derivative, TP-P1, which exhibits significantly improved aqueous solubility and safety profile. As a novel prodrug of triptolide (TP), TP-P1 markedly undergoes rapid and complete conversion to active TP in vivo. Compared with other TP derivatives such as Minnelide, TP-P1 exhibits superior pharmacokinetic properties and higher oral bioavailability. In animal models, TP-P1 demonstrates potent antitumor and anti-inflammatory activity with reduced toxicity and a broader therapeutic window. These advantages highlight TP-P1 as a promising candidate for further development and clinical translation.[16]

The TLR4/NF-κB pathway is a central regulator of inflammatory responses in rheumatoid arthritis, controlling the production of key pro-inflammatory cytokines such as TNF-α, IL-6, and IL-1β. Its aberrant activation in synovial fibroblasts, macrophages, and CD4+ T cells drives persistent inflammation and joint destruction, and TLR4-deficient mice are resistant to experimental arthritis.[17] These findings highlight the pathway's mechanistic and clinical relevance, justifying its focus as a therapeutic target in RA.

In this study, we developed a thermosensitive hydrogel formulation (TPTH) incorporating TP-P1 as the therapeutic agent and systematically evaluated its therapeutic efficacy in a collagen-induced arthritis (CIA) mouse model. Furthermore, we explored its underlying mechanisms from the perspectives of inflammation and oxidative stress. This work aims to provide a scientific foundation for the development of novel therapeutic formulations and targets for the treatment of rheumatoid arthritis.

Materials and Methods

Reagents and Instruments

Chitosan (CAS: 9012–76-4; molecular weight 190,000–375,000 Da) and β-Glycerophosphate disodium salt hydrate (CAS: 154804–51-0; molecular weight 216.04) were purchased from Sigma-Aldrich (USA); Primary antibodies included anti-TLR4 (19811-1-AP; Proteintech, China), anti-NF-κB p65 (66535-1-Ig; Proteintech, China) and anti-GAPDH (60004-1-Ig; Proteintech, China). Immunization Grade Bovine Type II Collagen (20022), Complete Freund's Adjuvant (7023) and Incomplete Freund's Adjuvant (7002) were purchased from Chondrex (USA).

Fabrication of Thermosensitive Chitosan Hydrogel

The thermosensitive chitosan hydrogel was prepared as previously described.[18] Briefly, chitosan (deacetylation degree ≥85%) was dissolved in 0.1 M acetic acid under magnetic stirring. A 56% (w/v) β-glycerophosphate (β-GP) solution was prepared in ultrapure water and gradually added to the chitosan solution under vigorous stirring at 4°C. The mixture was sterilized by autoclaving (15 min) and stored at 4°C until use. TPTH was prepared by combining the CS/β-GP solution with TP-P1 under gentle mixing until a homogeneous mixture was obtained.

Injectability Studies

The injectability of solutions of TPTH was assessed by observing thread-like hydrogel formation when the solution in a syringe was injected into a vial containing PBS solution at 37 °C.

Gelation Time

The gelation time was measured using the test tube inversion method in a constant-temperature water bath at 37 °C. For each sample, 1 mL was transferred into a test tube at room temperature and then incubated in the water bath. At 30 second intervals, the flowability of the sample was assessed by tilting the tube. The time point at which the sample ceased to flow was defined as the gelation time, and the corresponding value was recorded.

In vitro Release Study

For the in vitro release experiment, TPTH and free TP-P1 solution was loaded into a 1000 Da dialysis bag. The dialysis bag was immersed in a transparent vial containing 10 mL of PBS (pH 7.4) and placed on a shaker at 150 rpm under gentle, constant agitation. The release study was conducted at 37 °C, and at predetermined time intervals, the release medium was replaced with fresh PBS to maintain consistent release conditions. The amount of TP-P1 released was quantified using UV–visible spectrophotometry at 304 nm.

Cell Culture and Treatment

Mouse mononuclear macrophage leukemia cells (RAW264.7) were provided by Department of Hematology, Jiangsu Provincial Hospital of Traditional Chinese Medicine. RAW264.7 was cultured in DMEM medium (Gibco, USA) with 10% fetal bovine serum (FBS; Gibco, USA) in a 37°C incubator with a humidified atmosphere of 5% CO_2. RAW 264.7 macrophages were seeded in 24-well plates at a density of 5×10^4 cells per well. Cells were first stimulated with 1 μg/mL LPS for 24 hours, followed by treatment with DEX and hydrogel extracts for an additional 24 hours. After 24 h of cultivation, the total RNA of macrophage was extracted from each sample and the relevant gene expression was measured by RT-qPCR assay.

Experimental Animals

Male SPF-grade DBA/1J mice (*Mus musculus*, 6–8 weeks old, 18–22 g) were purchased from Jiangsu GemPharmatech Co., Ltd. (SCXK Su 2022–0070, Jiangsu, China) and housed under standard laboratory conditions: temperature 22 ± 2°C, relative humidity 60–80%, 12 h light/dark cycle, with ad libitum access to food and water. All procedures complied with the NIH Guide for the Care and Use of Laboratory Animals (Publication No. 8023) and were approved by the Ethics Committee of Nanjing University of Chinese Medicine (Approval No. 2024DW-024-01S).

Animal Grouping

Collagen-induced arthritis (CIA) was established as reported.[19] Bovine type II collagen (CII) was emulsified with an equal volume of complete Freund's adjuvant (CFA; Chondrex, USA) using a homogenizer on ice. Successful emulsification was confirmed by the absence of water dispersion upon droplet testing. The final CII concentration was adjusted to 1 mg/mL. For primary immunization, 100 μL of CII/CFA emulsion was intradermally injected at the tail base. On day 21, a booster immunization with CII emulsified in incomplete Freund's adjuvant (IFA) was administered at the same site. Control mice received saline. Post-modeling, mice were randomized into five groups (n = 6): Control (CTR), Model (MCG), Positive drug (MCG + DEX, 2mg/kg),[20] Blank hydrogel (Blank-H), Treatment (MCG + TPTH, 250μg/kg). The grouping and sample size are also consistent with previously published studies.[12,21] All treatments were administered via intra-articular injection every 4 days for 28 days. Clinical arthritis scores (AS) were assessed every 4 days. Mice were euthanized using an overdose of carbon dioxide, followed by collection of blood, knee, and ankle joints for analysis.

Paw Swelling and Arthritis Scoring

Right hind paw volume (PV) was measured every 4 days using a plethysmometer. A clinical scoring system was used to evaluate arthritis. (1) No sign of hyperemia or inflammation, the score is 0; (2) Little hyperemia with no paw swelling, the score is 1; (3) Modest hyperemia with swelling mainly localized in the ankle region, the score is 2; (4) The increased hyperemia and paw swelling in the ankle and metatarsal regions, the score is 3; (5) Significant hyperemia and paw swelling in the ankle, metatarsal and tarsal regions, the score is 4. The total score was calculated by summing the individual scores from both hind paws in each mouse.

Histopathological Staining

Knee joints and liver/kidneys were fixed in 4% neutral-buffered formalin (>48 h), paraffin-embedded, and sectioned (5 μm). Sections were stained with hematoxylin and eosin (H&E), safranin O-fast green (SO-FG), and Masson's trichrome using standard protocols. Images were acquired using a Nikon Eclipse Ni-U microscope (Japan).

Immunohistochemistry

Deparaffinized sections underwent antigen retrieval, endogenous peroxidase blocking (3% H_2O_2, 25 min), and blocking with 3% BSA (30 min). Primary anti-TLR4 antibody (1:100) was applied overnight at 4°C. After secondary antibody incubation (50 min, RT), DAB chromogen and hematoxylin counterstaining were performed. Sections were dehydrated and mounted with neutral resin.

Cytokine Quantification

EDTA-anticoagulated blood was centrifuged (1500×g, 10 min) to isolate plasma. Joint homogenates were centrifuged (1500×g, 10 min) to collect supernatants. Inflammatory cytokines were quantified using a multi-analyte flow assay kit (Biolegend, USA) on a Navios flow cytometer (RAISECARE, China). Data were analyzed with LEGENDplex v8 software.

Measurement of Anti-Type II Collagen Antibody Levels

Serum anti-type II collagen antibody (IgG) levels were measured using a commercial ELISA kit (Nanjing Youmeng Biotechnology Co., Ltd., China) according to the manufacturer's instructions. Absorbance was recorded at 450 nm with a microplate reader, and antibody concentrations were calculated based on the standard curve.

Quantitative Real-Time PCR (RT-qPCR)

Cell and Tissue RNA was extracted using a rapid RNA isolation kit (Feijie, China). cDNA was synthesized with 5× All-In-One RT Master Mix (Yugong Biotech, China). Primers and SYBR Green Master Mix (DBI Bioscience, China) were used for amplification on an ABI 7500 Real-Time PCR System (Thermo Fisher, USA). Relative mRNA expression was calculated via the $2^{-\Delta\Delta Ct}$ method, normalized to GAPDH. Experiments included triplicate replicates. Specific primers were synthesized by Sangon Biotech (Shanghai, China), with detailed sequences provided in Text S1.

Assessment of Oxidative and Antioxidant Biomarkers

Oxidative stress was evaluated by measuring malondialdehyde (MDA), a lipid peroxidation product, using an MDA assay kit (Beyotime, China) according to the manufacturer's protocol. Antioxidant capacity was determined through enzymatic activities of superoxide dismutase (SOD), catalase (CAT), and reduced glutathione (GSH) using commercial kits (Nanjing Jiancheng, China). Final concentrations were calculated based on standard formulas provided in the respective kits.

Western Blot Analysis

Joint tissue samples were homogenized with steel beads, and protein concentrations were quantified using a BCA assay. Equal amounts of protein (40 μg) were separated by 12.5% SDS-PAGE and transferred to PVDF membranes.

Membranes were blocked with protein-free rapid blocking buffer (PS108P, Epizyme, China) for 15 min at room temperature, followed by overnight incubation at 4°C with primary antibodies: TLR4 (1:1000), NF-κB (1:1000), and GAPDH (1:5000) (all from Proteintech, China). After incubation with HRP-conjugated secondary antibodies for 1 h at room temperature, protein bands were visualized using an ECL chemiluminescence reagent (P2300, NCM Biotech, China). Relative protein expression was analyzed using ImageJ software.

Safety and Biochemical Test

Systemic safety of drug treatment was assessed by analyzing plasma levels of aspartate aminotransferase (AST), alanine aminotransferase (ALT), creatinine (CRE), and blood urea nitrogen (BUN) in mice. Commercial assay kits (AST/GOT, ALT/GPT, CRE, BUN; Nanjing Jiancheng, China) were used strictly following the manufacturer's instructions. Plasma samples were incubated with specific reaction reagents, and absorbance of reaction products was measured using a microplate reader. Enzyme activities or metabolite concentrations were calculated based on standard curves. The in vitro cytocompatibility of the thermosensitive hydrogel was evaluated using RAW264.7 cells. Approximately 10% serum-containing culture medium was added to the hydrogel and incubated at 37 °C for 24 h to prepare the extraction medium, which was then sterilized using a 0.2 μm filter. RAW264.7 cells were seeded into 96-well plates at a density of 1×10^4 cells per well and incubated for 24 h at 37 °C in a humidified atmosphere containing 5% CO_2. The culture medium was then replaced with the hydrogel extraction medium, and the cells were further incubated for 24, 48, and 72 h. At the predetermined time points, cell viability was assessed using a microplate reader according to the CCK-8 assay protocol.

Statistical Analysis

Data are expressed as mean ± SEM. Statistical significance was determined using one-way or two-way ANOVA in GraphPad Prism 10. $p<0.05$ was considered statistically significant.

Results

TPTH Attenuates CIA-Induced Rheumatoid Arthritis in Mice

CS is the active ingredient extracted from chitosan and is a valuable natural product. As shown in Figure 1A, we prepared a thermosensitive TP-P1 hydrogel (TPTH). The hydrogel formulation flowed freely within the syringe. When injected into PBS (at 37°C), the contents smoothly exited the needle, forming a continuous thread-like soft gel that settled at the bottom of the vial without any phase separation or clumping. This indicates that the formulation is homogeneous, stable, and suitable as a thermosensitive injectable preparation (Figure 1B). The Blank-H and TPTH rapidly gelled within approximately 3 minutes, indicating quick gelation at body temperature. (Supplementary Figure 1). Free TP-P1 was completely released within 1 h, while TPTH showed a sustained release of 81% over 36 h (Supplementary Figure 2). A CIA-induced murine RA model was successfully established, with the experimental timeline illustrated in Figure 1C. To further confirm successful model induction, serum anti-type II collagen antibody levels were measured, which showed a significant increase in the model group and Blank-H (Supplementary Figure 3). The therapeutic efficacy of TPTH was evaluated in CIA mice through body weight monitoring, hind paw swelling measurement, and arthritis scoring, using dexamethasone (DEX) — a clinically established anti-inflammatory and analgesic agent — as the positive control. During the peak disease phase (days 29–33), model (MCG) and blank hydrogel (Blank-H) groups exhibited significant body weight loss ($p < 0.0001$ vs CTR, Figure 1D), accompanied by hind paw swelling ($p< 0.0001$ vs CTR, Figure 1E) and elevated arthritis scores compared to the control group (CTR) ($p< 0.0001$ vs CTR, Figure 1F). Macroscopic evaluation revealed pronounced hind paw edema and erythema in CIA mice (Figure 1E). Both TPTH and DEX markedly suppressed disease progression and paw swelling ($p < 0.0001$ vs MCG), whereas Blank-H showed no therapeutic effect. Histopathological analysis confirmed these findings: MCG and Blank-H groups exhibited cell proliferation, panus, cell erosion, inflammation and joint space narrowing, while TPTH and DEX maintained cartilage integrity and reduced synovial proliferation (Figure 1G and Supplementary Figure 4). Notably, there was no significant difference in efficacy between TPTH and DEX ($p > 0.05$), indicating comparable potency.

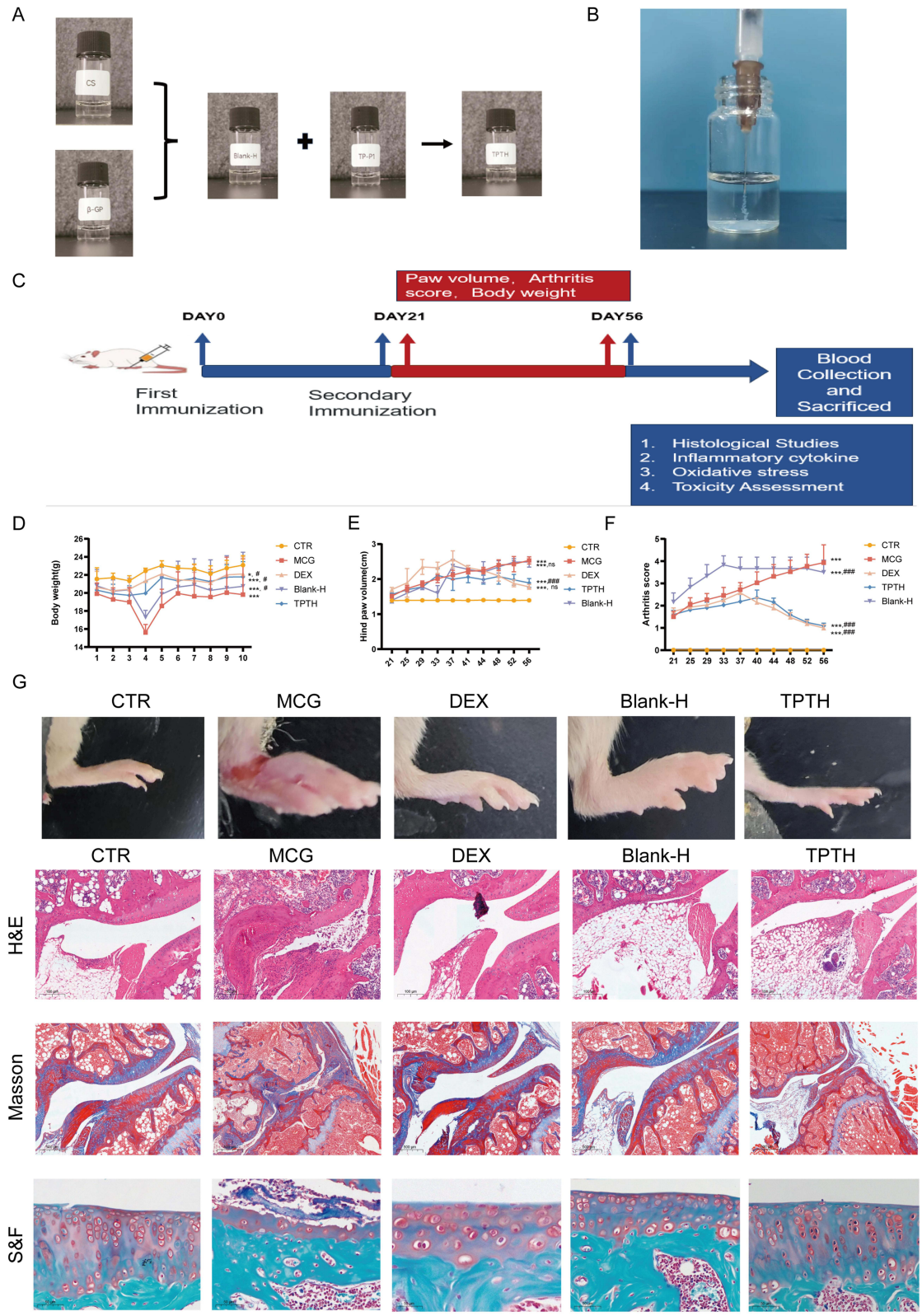

Figure 1 TPTH alleviates rheumatoid arthritis in CIA mice. (**A**) Schematic fabrication process of Thermosensitive TP-P1 Hydrogel. (**B**) Injectability of hydrogel studied under physiological conditions (37 °C and pH 7.4). (**C**) Schematic diagram of the animal experimental design. (**D**) Body weight changes of mice during the treatment period. (**E**) Swelling degree of the hind paws. (**F**) Clinical arthritis scores of the mice. (**G**) Representative images of paw swelling and histological sections of knee joints stained with H&E, Safranin O/Fast Green and Masson's trichrome. Scale bar: 50 μm per grid. Data are presented as mean ± SEM (n = 6). *$p < 0.05$, *** $p < 0.001$ vs CTR; $^{\#}p < 0.05$, $^{\#\#\#}p < 0.001$ vs MCG.
Abbreviations: CTR, healthy control group; MCG, model control group; DEX, dexamethasone positive control group; Blank-H, blank hydrogel group; TPTH, TP-P1 hydrogel group.

TPTH Reduces Proinflammatory Cytokine Levels in CIA Mice

To further evaluate the anti-inflammatory efficacy of TPTH, we assessed the expression levels of proinflammatory cytokines in both plasma and joint tissues of mice. Flow cytometry analysis revealed that levels of key proinflammatory cytokines, including IL-6, IL-23, IL-1 α, IL-1β, and TNF-α etc. were significantly elevated in the CIA model control group (MCG) compared to the normal group (Figure 2A and B). Notably, treatment with TPTH markedly attenuated the expression of these cytokines in both compartments. As a positive control, dexamethasone (DEX) also exerted a suppressive effect on the expression of these inflammatory mediators, albeit to a variable extent (Figure 2A and B). In addition, we examined the mRNA expression of selected cytokines in ankle and knee joint tissues. Compared with the normal group, CIA mice exhibited significantly increased mRNA levels of IL-6, IL-1β, and TNF-α, which were substantially downregulated following treatment with either TPTH or DEX (Figure 2C). Collectively, these results demonstrate that TPTH effectively suppresses the expression of multiple key proinflammatory cytokines in CIA mice, suggesting its potent immunomodulatory and anti-inflammatory properties.

TPTH Modulates Oxidative Biomarker Expression and Attenuates Oxidative Stress in CIA Mice

As shown in Figure 3, compared with the healthy control group, mice in the CIA model control group (MCG) exhibited increase in plasma malondialdehyde (MDA) levels, indicating enhanced lipid peroxidation and oxidative damage (Figure 3A). Concurrently, key antioxidant indicators, including catalase (CAT) activity, superoxide dismutase (SOD) activity, and glutathione (GSH) content, were reduced in the MCG group, reflecting impaired antioxidant defense and elevated oxidative stress (Figure 3B–D). In contrast, treatment with TPTH significantly reduced MDA levels while restoring CAT and SOD activities as well as GSH content, suggesting that TPTH effectively mitigates oxidative stress by both inhibiting oxidative damage and enhancing the endogenous antioxidant system. Similarly, dexamethasone (DEX) treatment also resulted in decreased MDA levels and improved antioxidant parameters. These findings indicate that TPTH alleviates oxidative damage in CIA mice by reducing the accumulation of oxidative products and enhancing antioxidant capacity, thereby contributing to its overall therapeutic efficacy.

TPTH Alleviates Joint Inflammation in CIA Mice via the TLR4/NF-κB Signaling Pathway

The TLR4/NF-κB signaling pathway plays a pivotal role in mediating inflammatory responses.[22] To further elucidate the anti-inflammatory mechanism of TPTH, we examined the expression levels of key components of this pathway using RT-qPCR, Western blotting and immunohistochemistry. Compared with the normal control group, the MCG group exhibited increased mRNA expression levels of TLR4, MyD88 and NF-κB in both cell and tissue samples (Figure 4A). As shown in Figure 4B, protein levels of TLR4 and its downstream effector NF-κB were elevated in the CIA model control group (MCG) compared to the healthy control group, indicating marked activation of this signaling axis in the disease state. Notably, treatment with TPTH significantly suppressed the expression of both TLR4 and NF-κB, suggesting that TPTH inhibits the activation of the TLR4/NF-κB pathway. These findings were further corroborated by immunohistochemical analysis, which demonstrated reduced TLR4 expression in joint tissues following TPTH treatment (Figure 4C). Collectively, these results suggest that the anti-inflammatory and antioxidative effects of TPTH are, at least in part, mediated through modulation of the TLR4/NF-κB signaling pathway.

In vivo Safety Evaluation of TPTH

To assess the in vivo biocompatibility of TPTH, histopathological analysis of liver and kidney tissues was performed using hematoxylin and eosin (H&E) staining. As shown in Figure 5A, the hepatic and renal tissue architecture in the TPTH-treated group remained intact, with no observable pathological alterations, indicating the absence of significant toxicity. Furthermore, we evaluated systemic toxicity by measuring plasma levels of key biochemical markers reflecting hepatic and renal function, including alanine aminotransferase (ALT), aspartate aminotransferase (AST), blood urea nitrogen (BUN), and creatinine (CRE). As shown in Figures 5B–E, the levels of ALT, AST, BUN, and CRE in the TPTH group were comparable to those of the healthy control group, suggesting that TPTH did not induce hepatic or renal

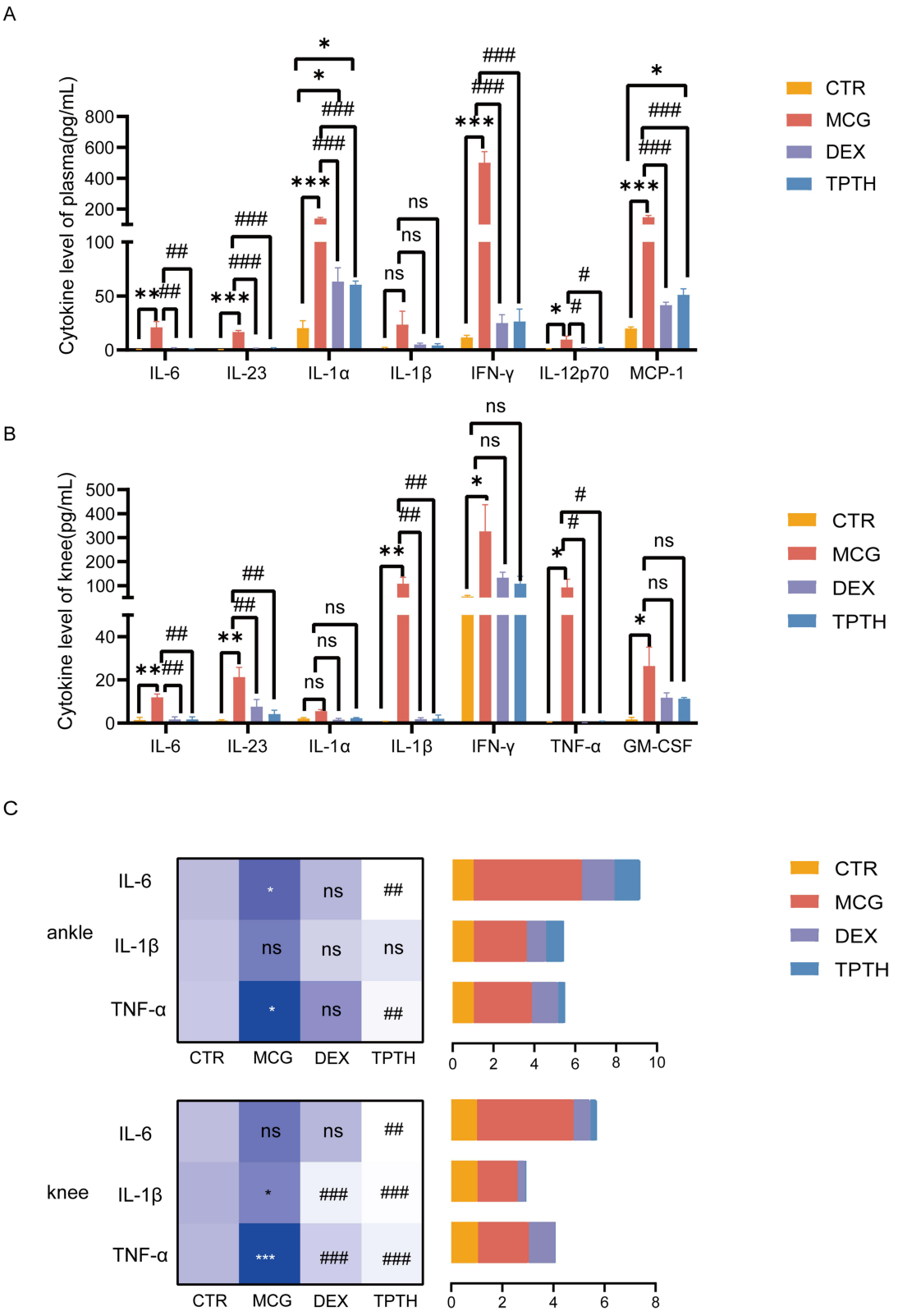

Figure 2 TPTH reduces proinflammatory cytokine levels in CIA mice. (**A**) The expression levels of proinflammatory cytokines in plasma. (**B**) The expression levels of proinflammatory cytokines in joint tissue. (**C**) The mRNA expression levels of IL-6, IL-1β, and TNF-α in ankle and knee joint tissues. Data are presented as mean ± SEM (n = 6). *$p < 0.05$, ** $p < 0.01$, *** $p < 0.001$ vs CTR; $^{\#}p < 0.05$, $^{\#\#}p < 0.01$, $^{\#\#\#}p < 0.001$ vs MCG.

Abbreviations: CTR, healthy control group; MCG, model control group; DEX, dexamethasone positive control group; Blank-H, blank hydrogel group; TPTH, TP-P1 hydrogel group.

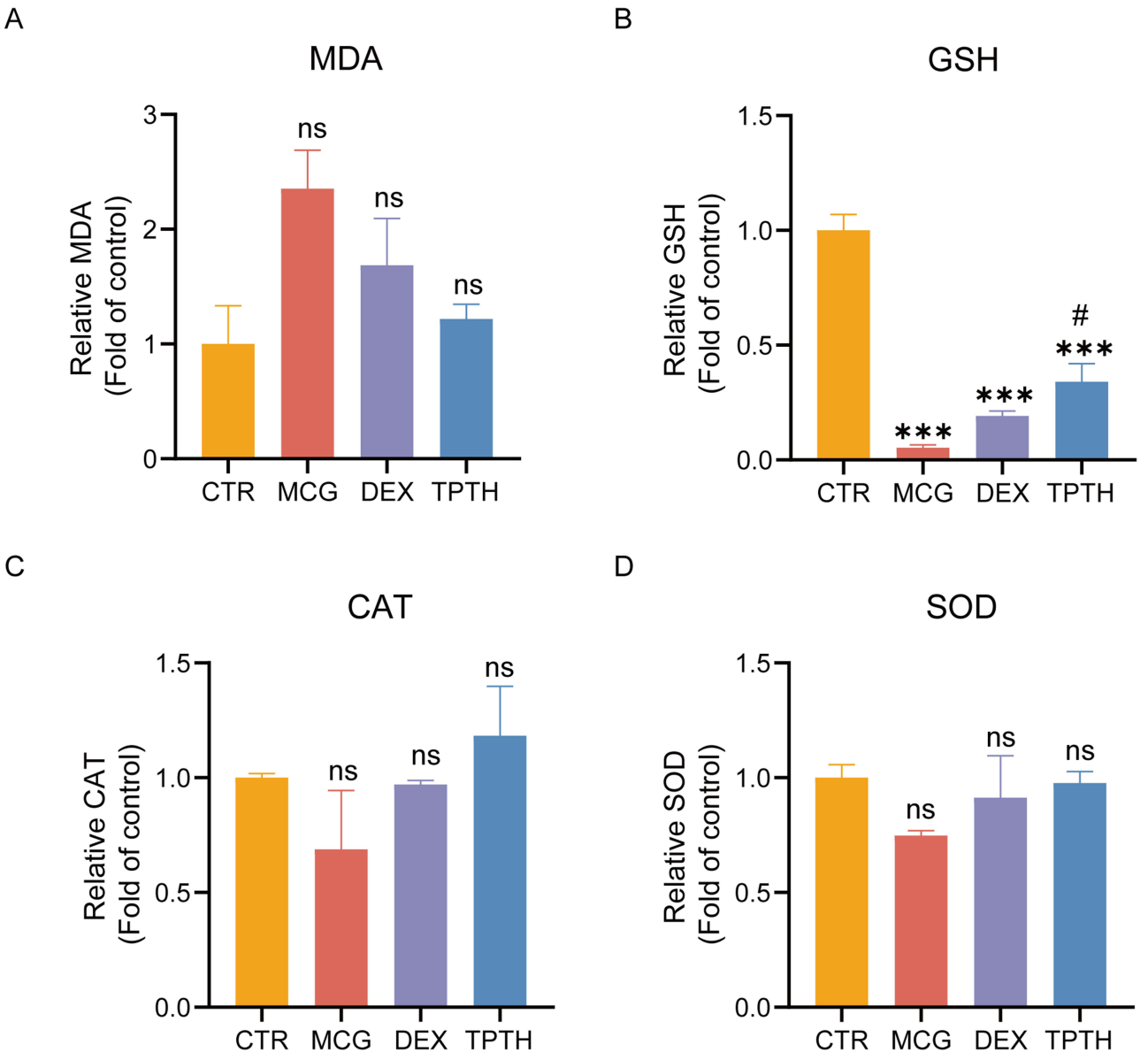

Figure 3 TPTH attenuates oxidative stress in CIA mice. (**A**) Malondialdehyde (MDA) levels in knee joint tissues. (**B**) Glutathione (GSH) levels in knee joint tissues. (**C**) Catalase (CAT) activity in knee joint tissues. (**D**) Superoxide dismutase (SOD) activity in knee joint tissues. Data are presented as mean ± SEM (n = 3). *** $p < 0.001$ vs CTR; # $p < 0.05$ vs MCG.

Abbreviations: CTR, healthy control group; MCG, model control group; DEX, dexamethasone positive control group; TPTH, TP-P1 hydrogel group.

injury. In the in vitro evaluation of biocompatibility, RAW264.7 cells were cultured in hydrogel extracts for 24, 48, and 72 hours, and cell viability was assessed using the CCK-8 assay (Supplementary Figure 5). At all three time points, cell viability remained above 90%, indicating that TPTH exhibited low cytotoxicity and further confirming its good cytocompatibility. Taken together, these results demonstrate that TPTH exhibits excellent biocompatibility both in vitro and in vivo, as well as favorable safety in CIA mice.

Discussion

Rheumatoid arthritis (RA) is a severe autoimmune disease and one of the most common types of systemic arthritis,[23] characterized by joint deformities, cartilage destruction, and persistent inflammation, RA has been described as a "cancer that never dies" and affects hundreds of millions of people worldwide.[24] Although nonsteroidal anti-inflammatory drugs (NSAIDs) and disease-modifying antirheumatic drugs (DMARDs) are currently the main therapeutic strategies for

https://doi.org/10.2147/JIR.S549625

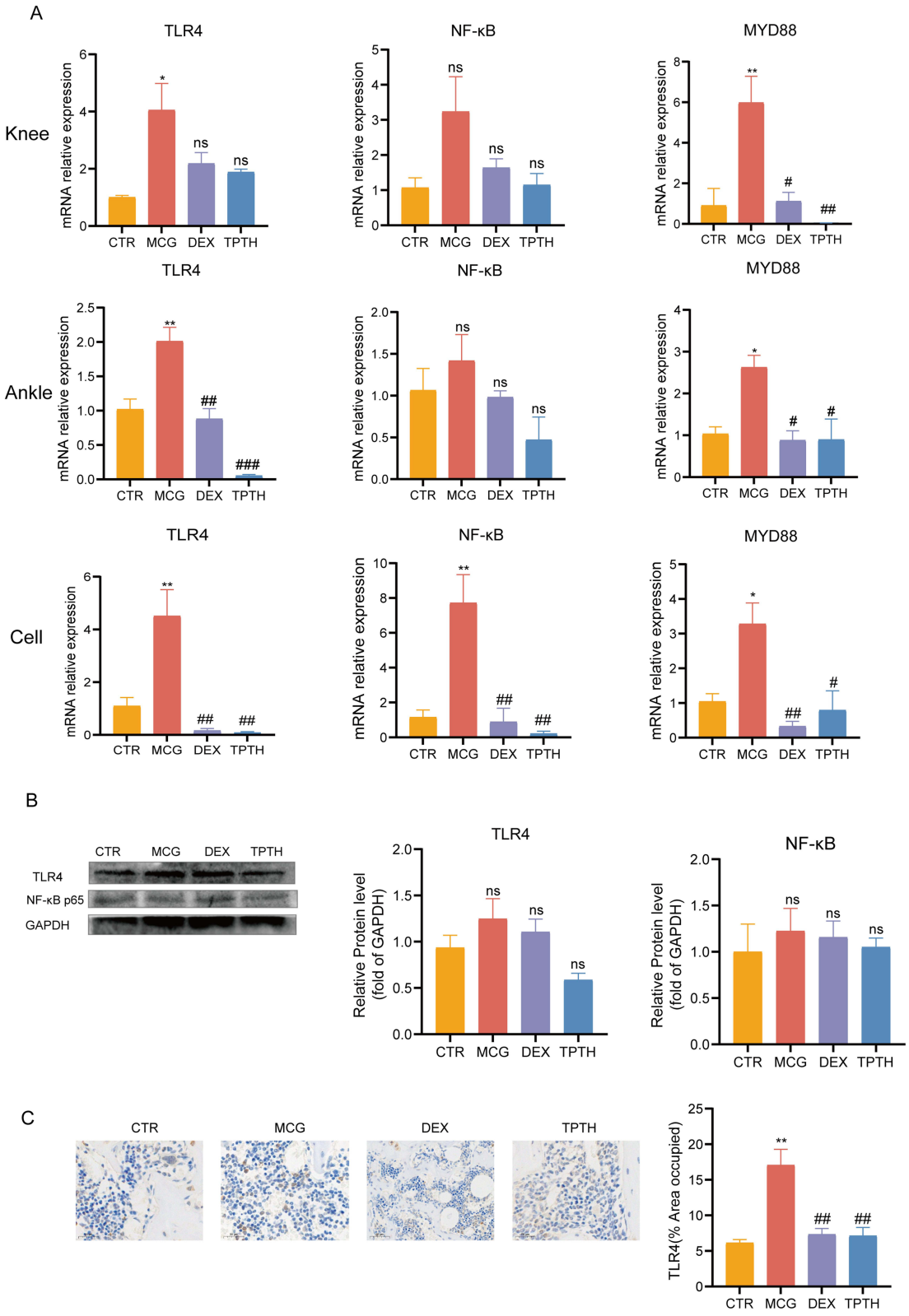

Figure 4 TPTH alleviates joint inflammation in CIA mice via the TLR4/NF-κB signaling axis. (**A**) mRNA expression levels of TLR4, MYD88 and NF-κB in knee, ankle joint tissues and cell. (**B**) Protein expression levels of TLR4 and NF-κB in knee joint tissues. (**C**) Representative immunohistochemical images of TLR4 expression in knee joint tissues and corresponding quantitative analysis. Data are presented as mean ± SEM (n = 3). *$p < 0.05$, ** $p < 0.01$ vs CTR; $^{\#}p < 0.05$, $^{\#\#}p < 0.01$, $^{\#\#\#}p < 0.001$ vs MCG. **Abbreviations**: CTR, healthy control group; MCG, model control group; DEX, dexamethasone positive control group; TPTH, TP-P1 hydrogel group.

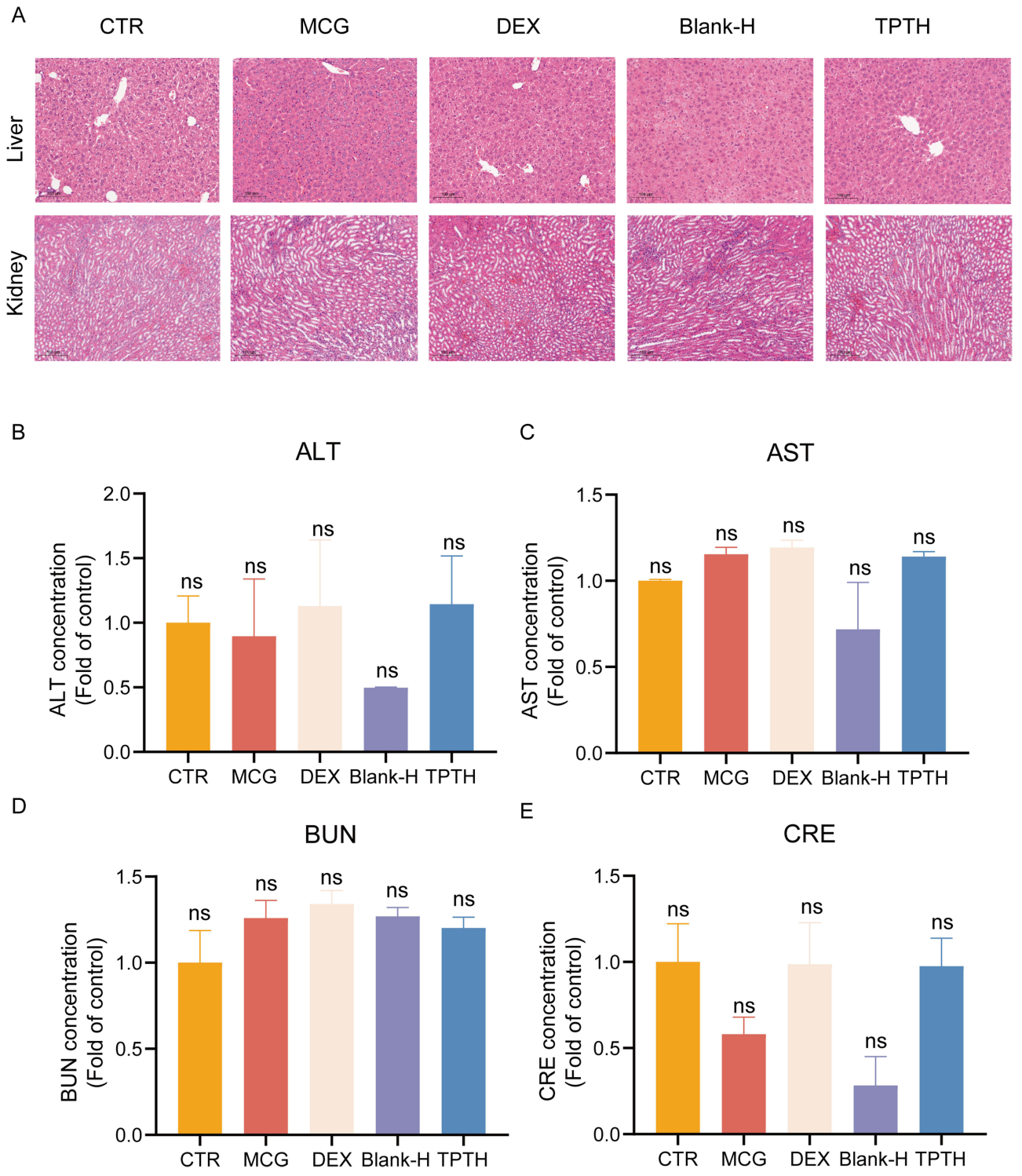

Figure 5 TPTH exhibited no significant toxicity in CIA mice. (**A**) Representative H&E staining images of liver and kidney sections from each group. (**B**–**E**) Plasma levels of liver and kidney function markers, including alanine aminotransferase (ALT), aspartate aminotransferase (AST), blood urea nitrogen (BUN), and creatinine (CRE), respectively. Data are presented as mean ± SEM (n = 3).

Abbreviations: CTR, healthy control group; MCG, model control group; DEX, dexamethasone-treated group; Blank-H, blank hydrogel group; TPTH, TP-P1 hydrogel-treated group.

https://doi.org/10.2147/JIR.S549625

managing RA progression, their widespread use is limited due to adverse side effects and high treatment costs. Therefore, there remains a significant clinical demand for safer, more affordable, and effective therapeutic approaches for RA.

The collagen-induced arthritis (CIA) mouse model is a well-established experimental model of immune-mediated inflammation and has been widely used for drug screening and mechanistic studies in RA research.[25] In the present study, the CIA model was used to simulate RA pathology. Consistent with previous reports,[26] mice in the model group exhibited pronounced inflammatory cell infiltration and cartilage destruction. In RA model evaluations, the arthritis score serves as a critical indicator of joint swelling severity. Due to sustained cellular infiltration and edema, mice in the model group displayed persistent joint swelling over 28 days. In contrast, the treatment groups exhibited peak swelling around day 7, followed by a gradual resolution of inflammation. Moreover, TPTH treatment significantly ameliorated body weight loss, hind paw swelling, and other RA-associated symptoms compared to the model control group (MCG), achieving therapeutic effects comparable to those of the positive control drug dexamethasone, indicating promising anti-RA potential of TPTH. Inflammation is widely recognized as a central mechanism and a key driver in the onset and progression of RA.[27]

Numerous pro-inflammatory cytokines are known to contribute to RA pathogenesis by promoting the generation of additional chemokines and cytokines at the pannus-cartilage interface, thereby exacerbating cartilage destruction. Interleukin-6 (IL-6) promotes B cell activation and proliferation, drives effector T cell-mediated tissue damage, and induces osteoclast differentiation, ultimately accelerating bone erosion and disease progression.[28] Tumor necrosis factor-alpha (TNF-α), another key inflammatory cytokine in RA, promotes osteoclastogenesis, inhibits osteoblast recruitment, and downregulates the expression of bone matrix–associated genes.[29] TNF-α also stimulates activated macrophages to release additional inflammatory mediators such as IL-6 and IL-1β, further amplifying the inflammatory response.[30,31] In addition to its established role in promoting inflammation, TNF has been shown to modulate mesenchymal stem cell (MSC) function in rheumatoid arthritis (RA). Recent studies indicate that TNF can influence MSC autophagy and apoptosis, thereby affecting tissue repair and immune homeostasis in RA joints.[32] Moreover, IL-1β is a classical serum biomarker of RA and is closely associated with disease severity.[33] Consistent with these findings, our study observed elevated levels of IL-6, IL-1β, and TNF-α in RA mice. Notably, TPTH treatment significantly reduced the plasma levels of these pro-inflammatory cytokines, supporting its potent anti-inflammatory efficacy.[34,35]

Oxidative stress also plays a vital role in the progression of painful RA and represents another key pathological feature of the disease.[36] Studies have shown that oxidative stress is markedly elevated in RA patients, potentially disrupting the body's natural antioxidant defense system and promoting the release of various pro-inflammatory cytokines and oxidative enzymes by immune cells, thereby intensifying autoimmune damage. Malondialdehyde (MDA), a lipid peroxidation product induced by free radicals, is widely recognized as a biomarker of oxidative damage, while superoxide dismutase (SOD) reflects the body's antioxidant capacity.[28] It has been reported that excessive accumulation of reactive oxygen species (ROS) impairs antioxidant defense mechanisms—including glutathione (GSH), catalase (CAT), and SOD—leading to elevated oxidative stress in RA.[37,38] Our current data similarly demonstrate increased plasma MDA levels and reduced CAT, SOD, and GSH levels in CIA mice, likely due to dysfunctional antioxidant defense systems failing to eliminate free radicals effectively.[39] Interestingly, TPTH-treated mice exhibited a marked reduction in MDA levels, accompanied by enhanced levels of CAT, SOD, and GSH, indicating the therapeutic potential of TPTH in alleviating oxidative stress-induced damage in RA.

The TLR4/NF-κB signaling pathway is critically involved in the pathogenesis of various inflammatory diseases, including RA. A growing body of evidence suggests that this pathway represents a potential therapeutic target for RA.[40,41] The progression of arthritis is closely linked to NF-κB, a key transcription factor activated downstream of TLR4. MyD88, a key adaptor protein downstream of TLR4, is essential for NF-κB activation through the MyD88-dependent pathway. Once activated, NF-κB not only promotes the inflammatory cascade but also contributes to bone loss, further aggravating joint destruction. Notably, NF-κB inhibitors have shown promising therapeutic effects in RA and are considered attractive candidates for clinical development.[42] In our study, both TLR4 and NF-κB expression were significantly upregulated in the MCG group, while TPTH treatment markedly reduced the expression of these pathway-associated proteins. These findings suggest that the anti-inflammatory effects of TPTH may be mediated, at least in part, through the inhibition of the TLR4/NF-κB signaling axis. This is consistent with findings reported by other researchers.

Interestingly, some studies also identified a decrease in the expression of pain-related genes, which provides a new direction for future investigations into the potential of this material in alleviating arthritis-associated pain.[43]

The sustained release properties and demonstrated efficacy of TPTH in preclinical models suggest promising potential for clinical translation. By maintaining therapeutic drug concentrations over an extended period, TPTH may reduce dosing frequency and minimize systemic side effects, which are common limitations of conventional TP therapy. Moreover, the local administration strategy could enhance target specificity, improving efficacy while limiting off-target toxicity. These findings provide a rationale for further development of TPTH as a safe and effective therapeutic option for rheumatoid arthritis and potentially other inflammatory diseases. Although this study demonstrated the potential of TPTH in suppressing inflammation and oxidative stress, certain limitations should be acknowledged, including the absence of gradient dosing and the relatively small sample size. In future studies, we plan to increase the sample size and include gradient doses to further investigate whether TPTH exhibits dose-dependent effects.

Conclusion

In summary, the thermosensitive hydrogel loaded with TP-P1 (TPTH) exhibits excellent anti-inflammatory and anti-oxidant properties, demonstrating great potential for the treatment of rheumatoid arthritis (RA). Within the pathological environment of RA—characterized by oxidative stress and extensive infiltration of inflammatory cells—this study highlights the protective role of TPTH in immune-mediated arthritis. In an inducible RA mouse model, TPTH significantly ameliorated multiple key pathological features of the disease, including reductions in arthritis index (AI), paw volume (PV), pro-inflammatory cytokine levels, and oxidative stress markers. These findings underscore the therapeutic promise of TPTH and suggest that TP-P1, a structurally modified derivative of Tripterygium wilfordii, holds considerable potential as a novel treatment for RA and other inflammation-related diseases associated with oxidative stress. These findings provide important insights for its potential clinical translation in patients with rheumatoid arthritis and expanded applications of such materials. Future studies will focus on evaluating the therapeutic effects of TPTH across different doses, exploring potential dose-dependent mechanisms, further assessing safety, and examining its translational potential in preclinical models.

Declaration of Generative AI and AI-Assisted Technologies in the Writing Process

During the preparation of this work, no AI or AI-assisted technologies were employed.

Abbreviations

RA, Rheumatoid Arthritis; CIA, Collagen-Induced Arthritis; TPTH, TP-P1-Loaded Thermosensitive Hydrogel; DEX, Dexamethasone; MDA, Malondialdehyde; GSH, glutathione; SOD, Superoxide dismutase; CAT, Catalase; ALT, Alanine Aminotransferase; AST, Aspartate Aminotransferase; BUN, Blood Urea Nitrogen; CRE, Creatinine; TLR4, Toll-Like Receptor 4; NF-κB, Nuclear Factor kappa-light-chain-enhancer of activated B cells.

Author Contributions

All authors made a significant contribution to the work reported, whether that is in the conception, study design, execution, acquisition of data, analysis and interpretation, or in all these areas; took part in drafting, revising or critically reviewing the article; gave final approval of the version to be published; have agreed on the journal to which the article has been submitted; and agree to be accountable for all aspects of the work.

Funding

This study was supported by the National Natural Science Foundation of China (82575012, 82001206, 81803942), the Science and Technology Planning Project of Jiangsu Province, China(BK20231375), the Key Disease Project of Jiangsu Province Hospital of Chinese Medicine (YZB2413), Developing Program for High-level Academic Talent in Jiangsu Hospital of Chinese Medicine (y2021rc42).

Disclosure

The authors report no conflicts of interest in this work.

References

1. Smolen JS, Aletaha D, McInnes IB. Rheumatoid arthritis. *Lancet*. 2016;388(10055):2023–2038. doi:10.1016/S0140-6736(16)30173-8
2. Burmester GR, Feist E, Dörner T. Emerging cell and cytokine targets in rheumatoid arthritis. *Nat Rev Rheumatol*. 2014;10(2):77–88. doi:10.1038/nrrheum.2013.168
3. van Vollenhoven RF. Treatment of rheumatoid arthritis: state of the art 2009. *Nat Rev Rheumatol*. 2009;5(10):531–541. doi:10.1038/nrrheum.2009.182
4. Aletaha D, Smolen JS. Diagnosis and management of rheumatoid arthritis: a review. *JAMA*. 2018;320(13):1360–1372. doi:10.1001/jama.2018.13103
5. Kesharwani D, Paliwal R, Satapathy T, Das Paul S. Rheumatiod arthritis: an updated overview of latest therapy and drug delivery. *J Pharmacopuncture*. 2019;22(4):210–224. doi:10.3831/KPI.2019.22.029
6. Sen R, Riofrio M, Singh JA. A narrative review of the comparative safety of disease-modifying anti-rheumatic drugs used for the treatment of rheumatoid arthritis. *Expert Opin Drug Saf*. 2024;23(6):687–714. doi:10.1080/14740338.2024.2348575
7. Esensten JH, Wofsy D, Bluestone JA. Regulatory T cells as therapeutic targets in rheumatoid arthritis. *Nat Rev Rheumatol*. 2009;5(10):560–565. doi:10.1038/nrrheum.2009.183
8. Ma T, Liu C, Zhao Q, Zhang Y, Xiao L. Decellularized nucleus pulposus matrix/chitosan hybrid hydrogel combined with nucleus pulposus stem cells and GDF5-loaded microspheres for intervertebral disc degeneration prevention. *Mol Med*. 2024;30(1):7. doi:10.1186/s10020-024-00777-z
9. Salehi S, Naghib SM, Garshasbi HR, Ghorbanzadeh S, Zhang W. Smart stimuli-responsive injectable gels and hydrogels for drug delivery and tissue engineering applications: a review. *Front Bioeng Biotechnol*. 2023;11:1104126. doi:10.3389/fbioe.2023.1104126
10. Gao C, Song XD, Chen FH, Wei GL, Guo CY. The protective effect of natural medicines in rheumatoid arthritis via inhibit angiogenesis. *Front Pharmacol*. 2024;15:1380098. doi:10.3389/fphar.2024.1380098
11. Lü S, Wang Q, Li G, Sun S, Guo Y, Kuang H. The treatment of rheumatoid arthritis using Chinese medicinal plants: from pharmacology to potential molecular mechanisms. *J Ethnopharmacol*. 2015;176:177–206. doi:10.1016/j.jep.2015.10.010
12. Yu GM, Zhou LF, Zeng BX, Huang JJ, She XJ. The antioxidant effect of triptolide contributes to the therapy in a collagen-induced arthritis rat model. *Redox Rep*. 2021;26(1):197–202. doi:10.1080/13510002.2021.2004047
13. Han R, Rostami-Yazdi M, Gerdes S, Mrowietz U. Triptolide in the treatment of psoriasis and other immune-mediated inflammatory diseases. *Br J Clin Pharmacol*. 2012;74(3):424–436. doi:10.1111/j.1365-2125.2012.04221.x
14. Xu H, Zhao H, Lu C, et al. Triptolide inhibits osteoclast differentiation and bone resorption in vitro via enhancing the production of IL-10 and TGF-β1 by Regulatory T cells. *Mediators Inflamm*. 2016;2016:8048170. doi:10.1155/2016/8048170
15. Fan D, He X, Bian Y, et al. Triptolide modulates TREM-1 signal pathway to inhibit the inflammatory response in rheumatoid arthritis. *Int J Mol Sci*. 2016;17(4):498. doi:10.3390/ijms17040498
16. Kang D, Pan X, Song Y, et al. Discovery of a novel water-soluble, rapid-release triptolide prodrug with improved drug-like properties and high efficacy in human acute myeloid leukemia. *Eur J Med Chem*. 2022;243:114694. doi:10.1016/j.ejmech.2022.114694
17. Singh JA, Saag KG, Bridges SL, et al. 2015 American college of rheumatology guideline for the treatment of rheumatoid arthritis. *Arthritis Rheumatol*. 2016;68(1):1–26. doi:10.1002/art.39480
18. Abrami M, Siviello C, Grassi G, Larobina D, Grassi M. Investigation on the thermal gelation of Chitosan/β-Glycerophosphate solutions. *Carbohydr Polym*. 2019;214:110–116. doi:10.1016/j.carbpol.2019.03.015
19. Brand DD, Latham KA, Rosloniec EF. Collagen-induced arthritis. *Nat Protoc*. 2007;2(5):1269-1275. doi:10.1038/nprot.2007.173.
20. Wahba MGF, Messiha BAS, Abo-Saif AA. Protective effects of fenofibrate and resveratrol in an aggressive model of rheumatoid arthritis in rats. *Pharm Biol*. 2016;54(9):1705–1715. doi:10.3109/13880209.2015.1125931
21. Huang S, Xu L, Wu Y, Chen K, Sun N, Feng Z. Orthogonal design-based investigation of dose, time point, and treatment course on the toxicity-efficacy transition of triptolide in collagen-induced arthritis mice. *Front Pharmacol*. 2025;16:1622570. doi:10.3389/fphar.2025.1622570
22. Shi P, Zhu W, Fu J, et al. Avicularin alleviates acute liver failure by regulation of the TLR4/MyD88/NF-κB and Nrf2/HO-1/GPX4 pathways to reduce inflammation and ferroptosis. *J Cell Mol Med*. 2023;27(21):3326–3338. doi:10.1111/jcmm.17905
23. Peng Y, Huang Y, Li H, et al. Associations between rheumatoid arthritis and intestinal flora, with special emphasis on RA pathologic mechanisms to treatment strategies. *Microb Pathog*. 2024;188:106563. doi:10.1016/j.micpath.2024.106563
24. Montoya T, Sánchez-Hidalgo M, Castejón ML, Rosillo MÁ, González-Benjumea A, Alarcón-de-la-Lastra C. Dietary oleocanthal supplementation prevents inflammation and oxidative stress in collagen-induced arthritis in mice. *Antioxidants*. 2021;10(5):650. doi:10.3390/antiox10050650
25. Wang Z, Zhang C, Meng J, et al. A targeted exosome therapeutic confers both CfDNA scavenging and macrophage polarization for ameliorating rheumatoid arthritis. *Adv Mater*. 2023;35(48):e2302503. doi:10.1002/adma.202302503
26. Wang G, Xie X, Yuan L, et al. Resveratrol ameliorates rheumatoid arthritis via activation of SIRT1-Nrf2 signaling pathway. *Biofactors*. 2020;46(3):441–453. doi:10.1002/biof.1599
27. Buch MH, Eyre S, McGonagle D. Persistent inflammatory and non-inflammatory mechanisms in refractory rheumatoid arthritis. *Nat Rev Rheumatol*. 2021;17(1):17–33. doi:10.1038/s41584-020-00541-7
28. Sun Y, Liu J, Xin L, et al. Xinfeng capsule inhibits inflammation and oxidative stress in rheumatoid arthritis by up-regulating LINC00638 and activating Nrf2/HO-1 pathway. *J Ethnopharmacol*. 2023;301:115839. doi:10.1016/j.jep.2022.115839
29. Yu H, Zeng R, Lin Y, et al. Kadsura heteroclita stem suppresses the onset and progression of adjuvant-induced arthritis in rats. *Phytomedicine*. 2019;58:152876. doi:10.1016/j.phymed.2019.152876
30. Joosten LAB, Netea MG, Dinarello CA. Interleukin-1β in innate inflammation, autophagy and immunity. *Semin Immunol*. 2013;25(6):416–424. doi:10.1016/j.smim.2013.10.018
31. Jing R, Ban Y, Xu W, et al. Therapeutic effects of the total lignans from Vitex negundo seeds on collagen-induced arthritis in rats. *Phytomedicine*. 2019;58:152825. doi:10.1016/j.phymed.2019.152825

32. Zhao Y, Yang X, Li S, et al. sTNFRII-Fc modification protects human UC-MSCs against apoptosis/autophagy induced by TNF-α and enhances their efficacy in alleviating inflammatory arthritis. *Stem Cell Res Ther*. 2021;12(1):535. doi:10.1186/s13287-021-02602-4
33. McInnes IB, Schett G. Pathogenetic insights from the treatment of rheumatoid arthritis. *Lancet*. 2017;389(10086):2328–2337. doi:10.1016/S0140-6736(17)31472-1
34. Lv Q, Wang K, Qiao S, et al. Norisoboldine, a natural AhR agonist, promotes Treg differentiation and attenuates colitis via targeting glycolysis and subsequent NAD+/SIRT1/SUV39H1/H3K9me3 signaling pathway. *Cell Death Dis*. 2018;9(3):258. doi:10.1038/s41419-018-0297-3
35. Chang JH, Chuang HC, Fan CK, Hou TY, Chang YC, Lee YL. Norisoboldine exerts antiallergic effects on IgE/ovalbumin-induced allergic asthma and attenuates FcεRI-mediated mast cell activation. *Int Immunopharmacol*. 2023;121:110473. doi:10.1016/j.intimp.2023.110473
36. López-Armada MJ, Fernández-Rodríguez JA, Blanco FJ. Mitochondrial dysfunction and oxidative stress in rheumatoid arthritis. *Antioxidants*. 2022;11(6):1151. doi:10.3390/antiox11061151
37. Li Y, Liang Q, Zhou L, et al. An ROS-responsive artesunate prodrug nanosystem co-delivers dexamethasone for rheumatoid arthritis treatment through the HIF-1α/NF-κB cascade regulation of ROS scavenging and macrophage repolarization. *Acta Biomater*. 2022;152:406–424. doi:10.1016/j.actbio.2022.08.054
38. Han Z, Gao X, Wang Y, et al. Ultrasmall iron-quercetin metal natural product nanocomplex with antioxidant and macrophage regulation in rheumatoid arthritis. *Acta Pharm Sin B*. 2023;13(4):1726–1739. doi:10.1016/j.apsb.2022.11.020
39. Das C, Bose A, Das D. Ayurvedic Balarista ameliorate anti-arthritic activity in adjuvant induced arthritic rats by inhibiting pro-inflammatory cytokines and oxidative stress. *J Tradit Complement Med*. 2021;11(3):228–237. doi:10.1016/j.jtcme.2020.04.006
40. Wang Y, Zheng F, Gao G, et al. MiR-548a-3p regulates inflammatory response via TLR4/NF-κB signaling pathway in rheumatoid arthritis. *J Cell Biochem*. 2019;120(2):1133–1140. doi:10.1002/jcb.26659
41. Arjumand S, Shahzad M, Shabbir A, Yousaf MZ. Thymoquinone attenuates rheumatoid arthritis by downregulating TLR2, TLR4, TNF-α, IL-1, and NFκB expression levels. *Biomed Pharmacother*. 2019;111:958–963. doi:10.1016/j.biopha.2019.01.006
42. Makarov SS. NF-kappa B in rheumatoid arthritis: a pivotal regulator of inflammation, hyperplasia, and tissue destruction. *Arthritis Res*. 2001;3(4):200–206. doi:10.1186/ar300
43. Wang QS, Xu BX, Fan KJ, Li YW, Wu J, Wang TY. Dexamethasone-loaded thermosensitive hydrogel suppresses inflammation and pain in collagen-induced arthritis rats. *Drug Des Devel Ther*. 2020;14:4101–4113. doi:10.2147/DDDT.S256850